

1

2 **Height correction of atmospheric motion vectors using airborne lidar observations**

3

4 Martin Weissmann, Kathrin Folger and Heiner Lange

5 *Hans-Ertel-Centre for Weather Research, Data Assimilation Branch, Ludwig-Maximilians-*

6 *Universität München, Germany*

7

8

9 Manuscript submitted to the *Journal of Applied Meteorology and Climatology*

10

11 February 2013

12

13

14 *Corresponding author address:*

15 Martin Weissmann,

16 LMU München, Meteorologie,

17 Theresienstr. 37,

18 80333 Munich, Germany

19 *E-Mail:* [martin.weissmann@lmu.de](mailto:martin.weissmann@lmu.de)

20 **ABSTRACT**

21       Uncertainties in the height assignment of Atmospheric Motion Vectors (AMVs) are the  
22 main contributor to the total AMV wind error and these uncertainties introduce errors that  
23 can be horizontally correlated over several hundred kilometers. As a consequence, only a  
24 small fraction of the available AMVs is currently used in numerical weather prediction  
25 systems. For this reason, we investigate how to improve the height assignment of AMVs, at  
26 first with airborne lidar observations and secondly by treating AMVs as layer-winds instead  
27 of winds at a discrete level.

28       Airborne lidar observations from a field campaign in the western North Pacific are used to  
29 demonstrate the potential of improving AMV heights in an experimental framework. On  
30 average, AMV wind errors are reduced by 10-15% when AMV winds are assigned to a 100-  
31 150 hPa deep layer beneath the cloud top derived from nearby lidar observations. In  
32 addition, the lidar-AMV height correction is expected to reduce the correlation of AMV  
33 errors as lidars provide independent cloud height information. This suggests that satellite  
34 lidars may be a valuable source of information for the AMV height assignment in the future.

35       Furthermore, AMVs are compared to dropsonde and radiosonde winds averaged over  
36 vertical layers of different depth to investigate the optimal height assignment for AMVs in  
37 data assimilation. Consistent with previous studies, it is shown that AMV winds better match  
38 sounding winds vertically averaged over ~100 hPa than sounding winds at a discrete level.  
39 The comparison to deeper layers further reduces the RMS difference, but introduces  
40 systematic differences of wind speeds.

41 **1. Introduction**

42 Atmospheric Motion Vectors (AMVs) derived by tracking the drift of cloud or water vapor  
43 features in satellite imagery are a key element of the global observing system for the  
44 initialization of numerical weather prediction (NWP) models. They particularly constrain the  
45 wind field in remote areas of the southern hemisphere and above the world's oceans where  
46 hardly any other wind observations exist. Several studies have documented the positive  
47 contribution of AMVs to the forecast skill of global NWP models (Bormann and Thépaut  
48 2004; Velden et al 2005; Gelaro et al. 2010). All major NWP centers now assimilate AMVs  
49 from several geostationary and polar orbiting satellites that together provide a nearly global  
50 coverage.

51 Despite improvements of the retrieval algorithms over the last decades however, the  
52 height assignment of AMVs introduces significant errors. Velden and Bedka (2009, VB2009  
53 hereafter) estimated that the height assignment is the dominant factor in AMV uncertainty  
54 and contributes up to 70% of the total error. In addition, those errors can be horizontally  
55 correlated over several hundred km (Bormann et al. 2003). As a consequence, AMVs are  
56 usually thinned rigorously for the assimilation in NWP models.

57 Spaceborne lidars as the one on the Cloud-Aerosol Lidar and Infrared Pathfinder Satellite  
58 Observation (CALIPSO) satellite can accurately determine the height of cloud tops.  
59 Therefore, the combination of AMVs with cloud top information from satellite lidars is seen  
60 as promising approach to reduce the error and error correlation of AMVs. Di Michele et al.  
61 (2012) compared cloud top heights derived from CALIPSO lidar data and AMV heights, but  
62 did not investigate the possibility of correcting AMV heights.

63 The present study intends to develop a height correction for AMVs based on lidar  
64 observations. Particular emphasis is given to investigate if the AMV should actually be  
65 assigned to the lidar observed cloud top itself or to some layer around or beneath the lidar  
66 cloud top observations. Instead of satellite lidar observations, the height correction is tested  
67 with airborne lidar observation during the The Observing System Research and Predictability  
68 Experiment (THORPEX) Pacific Asian Regional Campaign (T-PARC) 2008 (Weissmann et al.  
69 2011 and 2012). The use of airborne observations has the advantage that more than 300  
70 dropsondes are available to validate AMV winds before and after the correction.  
71 Observations of the lidar backscatter ratio at 1064 nm and dropsondes were performed  
72 during 24 research flights of the Falcon 20 research aircraft of the Deutsches Zentrum für  
73 Luft- und Raumfahrt (DLR).

74 In addition, the present paper investigates the appropriate layer depth and its vertical  
75 position for the assimilation of AMVs. The study of VB2009 indicates that AMVs represent  
76 the wind in a tropospheric layer rather than at a finite level. For this reason they calculated  
77 the vector root-mean-square (VRMS) difference between AMVs and radiosonde winds  
78 averaged over layers of different depth from the AMV height downward. The present paper  
79 additionally investigates the effect of layer-averages on the wind speed bias as systematic  
80 errors are particularly crucial in data assimilation. Furthermore, we test different vertical  
81 positions of the averaging layer relative to the original AMV height. For this purpose we  
82 compare AMVs to sounding winds averaged over layers of different depth and we shift these  
83 layers from above to beneath the AMV. Systematic wind speed differences are calculated in  
84 addition to VRMS differences as deeper layers lead to systematically weaker winds. The  
85 comparison is based on several thousand vertical soundings (dropsondes and special  
86 radiosondes from ships and small islands) during T-PARC.

87 The paper is outlined as follows: Section 2 describes T-PARC and the data set. Section 3  
88 first compares AMV heights to lidar cloud top heights and then evaluates an AMV height  
89 correction using lidar observations. Section 4 compares AMVs to layer-averaged radiosonde  
90 and dropsonde winds and section 5 discusses and summarizes the results.

91

## 92 **2. Data set**

### 93 ***a. T-PARC observations***

94 The summer component of the multinational T-PARC field campaign was conducted in  
95 August to October 2008 in the western North Pacific. T-PARC and the associated projects  
96 Tropical Cyclone Structure 2008 (TCS-08) and Dropwindsonde Observations for Typhoon  
97 Surveillance near the Taiwan Region (DOTSTAR) aimed to investigate the genesis of tropical  
98 cyclones (TCs), to improve typhoon track and intensity forecasts by targeted observations  
99 and to investigate the extratropical transition of TCs and their downstream impact in  
100 midlatitudes (for more information see: <http://www.eol.ucar.edu/projects/t-parc/>). The  
101 main observational platforms were four research aircraft launching dropsondes: The German  
102 DLR Falcon 20, the U.S. Navy P-3, the U.S. Air Force WC-130 and the Taiwanese DOTSTAR  
103 Astra Jet. Altogether, over 500 flight hours were spent and over 1300 dropsondes were  
104 launched in a period from 1 August to 3 October 2008. In addition to dropsondes, additional  
105 radiosondes were launched from Japanese research vessels and from small islands. The right  
106 panel of Fig. 1 shows the location of radiosondes and dropsondes used for the comparison of  
107 AMVs with layer-averaged sounding winds in section 4.

108 The DLR Falcon was additionally equipped with a scanning wind lidar and a differential  
109 absorption lidar (DIAL) system for water vapor observations (Wirth et al. 2009; Harnisch et  
110 al. 2011). As a byproduct of water vapor profiles, the DIAL system also observes vertical  
111 profiles of the backscatter ratio (*BSR*) beneath the aircraft at a wavelength of 1064 nm.  
112 These profiles can be used to accurately determine the height of cloud tops. After testing  
113 different approaches for deriving cloud top heights, the maximum of the *BSR* gradient plus a  
114 threshold for the *BSR* gradient were used for cloud detection. There are many different  
115 approaches for deriving cloud tops from lidar observations, but in general it was found that  
116 the differences between cloud heights derived using different approaches or slightly  
117 modified thresholds are clearly smaller than the differences between lidar cloud top heights  
118 and AMV heights (see Folger 2012 for details of the applied cloud detection method and  
119 differences of several approaches). The average horizontal resolution of the lidar  
120 observations is about 2 km. As AMVs are derived from a significantly larger area, the median  
121 of all cloud top heights derived from lidar observations within 100 km distance and 60 min  
122 time difference is used for the comparison with AMV heights and the correction of these  
123 heights. The DLR Falcon performed 24 research flights with dropsonde and lidar *BSR*  
124 observations during T-PARC (left panel in Fig. 1). About 50 flight hours with lidar *BSR*  
125 observations were available for the AMV height correction after quality screening.

126 The Cooperative Institute for Meteorological Satellite Studies (CIMSS) produced an  
127 experimental data set for T-PARC consisting of hourly AMVs from images of the operational  
128 Japanese Multi-functional Transport Satellite 1R (MTSAT-1R) in four channels: (a) infra-red  
129 (IR) observations at 10.8  $\mu\text{m}$ ; (b) visible (VIS) observations at 0.73  $\mu\text{m}$  for daytime low  
130 clouds; (c) shortwave infra-red (SWIR) observations at 3.75  $\mu\text{m}$  for nighttime low clouds; (d)  
131 observations in a channel sensitive to water vapor. The present study uses AMVs in the first

132 three channels (IR, VIS and SWIR) that track clouds features. The CIMSS algorithm for  
133 deriving AMVs is close to that used operationally by the National Environmental Satellite,  
134 Data, and Information Service (NESDIS) of the National Oceanic and Atmospheric  
135 Administration (NOAA). The size of the target box for deriving VIS and IR AMVs was 15x15  
136 pixels (about 60 km) and the target box for SWIR AMVs was 7x7 pixels (about 28 km). AMV  
137 heights were determined using the H<sub>2</sub>O intercept method, the IR histogram method, and  
138 the cloud base method (see Nieman 1993 and Olander 2001 for more details). The first two  
139 methods estimate the cloud top height (as the lidar observations) whereas the last one  
140 estimates the cloud base height. On average, the cloud base method was applied for about  
141 one quarter of AMVs beneath 600 hPa.

142 The mean flight level of the DLR Falcon was 11 km ASL, but lidar cloud observations  
143 within 150 hPa from the aircraft downward were not used to assure that no AMVs from  
144 clouds above the aircraft with a lower erroneous height assignment appear in the data set.  
145 Due to this selection criterion and a minimum of the number of cloud AMVs in the middle  
146 troposphere, only AMVs beneath 500 hPa are used for the height comparison and height  
147 correction. As a consequence, all AMVs in the resulting data set were derived from water  
148 clouds, but not from ice clouds. About 50% of these AMVs are VIS, about 30% are SWIR and  
149 20% are IR (Fig. 2). The low fraction of IR AMVs is due to the fact that those are mainly  
150 located at higher altitudes. SWIR AMVs are only derived during nighttime, whereas most  
151 flights were performed during daylight.

152

153 ***b. Selection criteria for observations***

154 Observations for the lidar-AMV height comparison and correction in section 3 were  
155 selected with the condition that there are at least 10 lidar cloud observations within 60 min  
156 time difference and 100 km horizontal distance from an AMV. A representative cloud top  
157 height is then derived from these lidar observations by taking the median of all individual  
158 lidar cloud top observations. Whenever the rms of differences between the individual  
159 observations and the median exceeds 70 hPa, the observations are discarded. CIMSS also  
160 provides a quality indicator (QI) for AMVs that ranges from 0-100 with 100 indicating the  
161 highest quality. This QI must be at least 50 for observations used in section 3. These  
162 thresholds were chosen to exclude lidar observations and AMVs from different clouds  
163 without reducing the sample size too much.

164 In addition, the height comparison in section 3a applied the criterion that the AMV height  
165 and the lidar cloud top must be within 150 hPa vertically to discard values where AMVs and  
166 the lidar cloud signal come from clouds at very different heights due to the temporal or  
167 horizontal displacement of the observations. Applying these criteria resulted in 656 AMVs  
168 with nearby lidar cloud top observations heights for the comparison.

169 For the AMV height correction using lidar observations in section 3b, the pressure  
170 difference criterion was replaced by the criterion that the applied height correction is not  
171 more than 100 hPa, i.e. the center of the layer that the AMV is shifted to must be within 100  
172 hPa from the original AMV height. This criterion is based on the assumption that AMV height  
173 errors are usually less than about 100-150 hPa, on sensitivity studies with different limits  
174 and the visual comparison of lidar *BSR* cross-sections and AMV heights. The evaluation of the  
175 lidar-AMV height correction was performed with wind observations from the two nearest



176 dropsondes released by the DLR Falcon. Only one dropsonde was used for the first and last  
177 observations of a flight. For this evaluation, the additional criterion was applied that there is  
178 at least one dropsonde within 100 km and 60 min from the AMV and the lidar observations  
179 used for the correction. 369 data matches were available that fulfilled the collocation  
180 criterion for dropsondes, AMVs and lidar observations for the height correction. About one  
181 quarter of these was discarded by the pressure difference criterion.

182 The comparison of AMVs to layer-averaged radiosonde and dropsonde winds in section 4  
183 applied the same threshold for temporal and horizontal displacement that was used in  
184 section 3 (100 km and 60 min), but the threshold for the CIMSS QI was increased to 70 as the  
185 data set was significantly larger and therefore allowed a more rigorous limit. Altogether  
186 13,000 matches of AMVs and sounding winds are used in section 4.

187

### 188 **3. Lidar-AMV height comparison and correction**

#### 189 ***a. Height comparison***

190 The histogram of height differences between AMVs and representative lidar cloud tops is  
191 shown in Fig. 3. Representative lidar cloud tops for every AMV are derived by taking the  
192 median of all lidar cloud top observations within 100 km and 60 min from the respective  
193 AMV as described in section 2. The distribution strongly depends on the AMV type. VIS  
194 AMVs are distributed throughout the vertical range of +/- 150 hPa from the lidar cloud top  
195 height with more AMVs above than beneath the lidar cloud top. The majority of IR AMVs  
196 and nearly all SWIR AMVs in contrast are located beneath the lidar cloud tops. On average,  
197 the pressure of VIS AMVs is 21 hPa lower than at the lidar cloud tops, which means that VIS

198 AMVs are on average located higher than the lidar cloud tops. The pressure of IR AMVs is 15  
199 hPa higher than at the lidar cloud top and the pressure of SWIR AMVs is 53 hPa higher.

200 The important question is where AMVs should be located relative to the lidar cloud top as  
201 AMVs may represent the wind in a layer beneath the cloud top. In that case, the AMV height  
202 should actually be lower than the lidar cloud top observations. For this reason, we computed  
203 the mean VRMS differences between the AMVs shown in Fig. 3 and layer-averaged  
204 dropsonde winds to aid the interpretation of systematic height differences. Once, the  
205 dropsonde wind is averaged over a layer starting at the AMV height and going downward by  
206 50, 100 or 150 hPa (also referred to as comparing or assigning a layer beneath hereafter)  
207 and secondly, the wind is averaged over a layer of the same depth centered at the original  
208 AMV height. In case such a layer extends beneath the ground level, the layer depth is  
209 reduced accordingly to end at ground level. Mean VRMS differences are calculated as the  
210 mean of the square-root of the sum of the squared differences of both wind components.  
211 Fig. 4 shows the relative reduction of mean VRMS differences when a layer beneath the  
212 AMV height is compared instead of a layer of the same depth centered at the AMV height.

213 For VIS AMVs, the mean dropsonde-AMV VRMS difference is 9-15% lower when  
214 dropsonde winds are averaged over layers beneath the original AMV height than for  
215 averaging over layers of the same depth centered at the original AMV height (Fig. 4). The  
216 reduction is significant at the 99% confidence level for layer depths of 50, 100 and 150 hPa  
217 using a Student's t-test for dependent samples. This indicates that VIS AMVs are clearly too  
218 high as the center of these layers is 25-75 hPa beneath the original AMV height.

219 The differences of SWIR AMVs and dropsondes are also reduced when dropsonde winds  
220 are averaged over layers of 100-150 hPa beneath the original AMV although those AMVs are

221 already located 53 hPa beneath lidar cloud tops on average. The AMV-dropsonde differences  
222 for IR AMVs in contrast, increase by nearly 10% for 150 hPa layers beneath the original AMV  
223 height. However, the reduction or increase of mean VRMS differences is not significant for  
224 both IR and SWIR AMVs. Further discussion of the optimal layer assignment relative to the  
225 original AMV height based on a much larger sample size is presented in section 4, whereas  
226 the purpose of Fig. 4 is only to aid the interpretation of differences between AMV and lidar  
227 cloud top observations shown in Fig. 3.

228 Overall, we conclude that AMV heights should be located lower than lidar cloud tops. VIS  
229 AMVs are on average located 21 hPa above lidar cloud tops, but they appear to represent  
230 winds in a layer that is centered 50-75 hPa lower than their current height and therefore  
231 29-54 hPa lower than lidar cloud tops. IR and SWIR AMVs are already located 15 and 53 hPa  
232 beneath lidar cloud tops, respectively.

233

#### 234 ***b. Height correction***

235 This section describes the correction of AMV heights with airborne lidar cloud top  
236 observations and the evaluation of wind differences to dropsondes before and after the  
237 height correction. The correction shifts the AMV wind vertically to a layer relative to the  
238 median height of a nearby lidar cloud top observations (see section 2 for the description of  
239 the data set and selection criteria). Fig. 5 shows the differences of AMV and dropsonde  
240 winds using different layer depths and three different layer positions relative to the lidar  
241 cloud top observations for the correction. Mean VRMS differences generally decrease with  
242 increasing layer depth. The lowest mean VRMS difference is reached when AMVs are shifted  
243 to a layer from the lidar cloud top to 100-150 hPa beneath or, in other words, when AMV

244 winds are compared to dropsonde winds averaged over a layer from the lidar cloud top to  
245 100-150 hPa beneath. Assigning a 150 hPa layer that is 25% above and 75% beneath the lidar  
246 cloud tops leads to about the same result. The bias is less than  $0.2 \text{ m s}^{-1}$  for all layer depths  
247 and position that were tested. Results for the individual channels (VIS, IR and SWIR, not  
248 shown) are similar and in general it seems best to assign AMVs to 100-150 hPa deep layers  
249 beneath the lidar cloud top or to 150 hPa layers with 25% above and 75% beneath the lidar  
250 cloud top.

251 Fig. 6 shows the relative improvement, i.e. relative reduction of mean VRMS differences  
252 between AMV and dropsonde winds for assigning AMV winds to a layer of 100 or 150 hPa  
253 beneath the lidar cloud top observation instead of a layer of the same depth centered at  
254 their original height. On average, this height correction reduces VRMS differences by 14%.  
255 The average error reduction is largest for IR AMVs (14-19%), followed by VIS AMVs (~16%)  
256 and SWIR AMVs (9-11%). The reduction is statistically significant at the 99% confidence level  
257 for all AMVs and the subsets of VIS and SWIR AMVs. The reduction of the IR subset is  
258 significant at the 95% confidence level.

259 As shown in section 3a, the errors of VIS AMVs are also reduced by ~14%, when a layer  
260 beneath the original AMV height is assigned. However, the optimal layer relative to the  
261 original AMV height likely depends on the AMV data set and processing, whereas the lidar  
262 information is independent of the AMV processing. For SWIR and IR AMVs, the lidar  
263 correction leads to clearly lower errors than assigning a layer beneath the original AMV  
264 height. Further discussion on the potential of reducing AMV errors through assigning a layer  
265 relative to the original AMV height is provided in the following section.

266

#### 267 **4. Comparing AMVs to layer-averaged radiosonde and dropsonde winds**

268 Section 3a suggests that the error of VIS AMVs is substantially reduced when they are  
269 assigned to a layer beneath their original height and section 3b demonstrates that the error  
270 of AMVs in all channels is reduced when a layer beneath lidar cloud top observations is  
271 assigned to them. These results motivated a further investigation of how deep the  
272 atmospheric layer is that AMVs represent and how this layer should be positioned vertically  
273 if no additional lidar information is available. To increase the sample size, this section uses  
274 dropsondes from all four T-PARC aircraft and special T-PARC radiosondes. The use of  
275 radiosondes also allows comparing AMVs at altitudes of 100-500 hPa, whereas the section 3  
276 only uses AMVs beneath 500 hPa.

277 VB2009 already compared VRMS differences between AMV winds and layer-averaged  
278 sounding winds for layers of different depth from the AMV height downward. Their results  
279 suggest that the treatment of AMVs as layer-averaged winds beneath their original height in  
280 data assimilation could lead to a significant improvement. This section intends to  
281 complement the study of VB2009 by testing different positions of the layer relative to the  
282 original AMV height and by investigating the effect on the wind speed bias in addition.

283 Assigning a layer beneath the original AMV height results in a systematic height reduction  
284 and may therefore introduce systematic wind errors in case the height was correct or too  
285 low before. A larger averaging volume additionally leads to lower wind speeds. As data  
286 assimilation systems are particularly sensitive to systematic errors, we investigate the wind  
287 speed bias in addition to VRMS differences and we shift the averaging layers from 50 or 100  
288 hPa above the AMV height to 100 hPa beneath. Whenever the averaging layer would extend  
289 beneath the ground, we use the lowest possible layer instead. The intention for shifting the

290 layer is to find the optimal position of the layer relative to the AMV height and also to detect  
291 if the reduction of the difference is due to compensating systematic height errors by  
292 extending the layer to the correct height of the AMV wind or to the fact that AMVs really  
293 represent a layer wind.

294 The VRMS differences and the wind speed bias between AMV winds and layer-averaged  
295 sounding winds is shown in Fig. 7 for different layer depths (different line types) as a  
296 function of the vertical offset of the center of the averaging layer relative to the AMV height.  
297 The line type with the lowest minimum indicates the optimal (or appropriate) layer depth  
298 concerning mean VRMS or wind speed bias. The position of this minimum on the x-axis  
299 indicates the optimal (or appropriate) position of the layer relative to the AMV height. The  
300 fact that the line with the lowest VRMS minimum is also the one with the lowest VRMS value  
301 at  $x=0$  hPa in all panels indicates that the compensation of systematic height errors is not the  
302 main effect for the VRMS reduction.

303 The results for IR AMVs above 499 hPa indicate that the lowest mean VRMS difference is  
304 reached when these AMV are assigned to a 100 hPa layer centered  $\sim 20$  hPa beneath their  
305 original height. Deeper or shallower layers both lead to larger differences. However, a 50  
306 hPa layer centered 16 hPa beneath the original AMV height may be the best choice in case a  
307 low wind speed bias is particularly important.

308 AMVs beneath 500 hPa (Figs. 7b-f) generally show a less distinct minimum of VRMS  
309 differences, presumably due to lower vertical wind gradients at lower levels. The lowest  
310 mean VRMS differences are generally reached for the deepest layer that is shown, i.e. for  
311 200 hPa. Averaging over these layers however leads to an increase of the wind speed bias

312 that may not be desirable for data assimilation purposes. Thus, the choice of the optimal  
313 (appropriate) layer is to some extent a trade-off between mean VRMS and bias.

314 The mean VRMS difference is systematically reduced by 0.2-0.4 m s<sup>-1</sup> when AMVs are  
315 assigned to a 100 hPa layer centered at their original height instead of a 10 hPa layer  
316 centered at that height (upper part in Table 1). Assigning such a layer also does not seem to  
317 lead to a significant increase of the wind speed bias. Table 1 also lists the mean VRMS and  
318 bias difference for one subjectively chosen optimal layer for every panel of Fig. 7 (lower part  
319 in Table 1). 150 and 200 hPa layers were not selected due to the increase of the wind speed  
320 bias mentioned above. It is notable that these optimal layers are sometimes centered above  
321 and sometimes beneath the original AMV height in contrast to the assumption of VB2009  
322 that layers beneath the AMV level are appropriate. The results in Fig. 7 suggest that a layer  
323 centered at the AMV height may be the best choice for all AMVs above 799 hPa. Only for VIS  
324 and SWIR AMVs beneath 800 hPa, there is indication that assigning a 100 hPa layer beneath  
325 the original AMV height is more appropriate as both the mean VRMS and bias are reduced.  
326 For VIS AMVs beneath 800 hPa, such a layer beneath the original height even leads to lower  
327 VRMS differences than a layer at the original AMV height while the wind speed bias is about  
328 the same. For SWIR AMVs beneath 800 hPa, mean VRMS and bias for the layer beneath are  
329 comparable to the values for the layer centered at the original AMV height.

330

## 331 **5. Discussion and summary**

332 This study develops a method for correcting lower tropospheric AMV heights with  
333 airborne lidar cloud top observations and investigates if AMVs rather represent winds in a  
334 layer instead of at a distinct level. The field campaign T-PARC in the western North Pacific

335 offered a unique opportunity for such an investigation as it provided an experimental data  
336 set of hourly MTSAT AMVs produced by CIMSS, airborne lidar observations from 24 flights of  
337 the DLR Falcon, more than 300 dropsondes from the same flights for an independent  
338 evaluation of the AMV height correction using lidar observations and several thousand  
339 additional soundings for the comparison of AMVs to layer-averaged winds. The lidar-AMV  
340 height comparison and correction are limited to AMVs beneath 500 hPa due to the aircraft  
341 flight altitude, whereas the layer comparison also includes AMVs up to 100 hPa.

342 The first part of the study demonstrates that lower tropospheric AMV heights can be  
343 corrected using airborne lidar observations. The best match of AMV and dropsonde winds is  
344 found when AMVs are assigned to 100 or 150 hPa deep layers beneath the median of cloud  
345 top heights derived from nearby lidar observations. On average, the wind error of AMVs is  
346 reduced by 10-15% when AMVs are assigned to layers beneath the median of lidar cloud  
347 tops instead of layers centered at the original AMV height. The reduction is even larger when  
348 AMV-dropsonde differences at a discrete level are used as reference. Vertical layers with  
349 75% beneath and 25% above the median of lidar cloud tops lead to similar results. The  
350 improvement is consistent for all channels (VIS, SWIR and IR) and the results are statistically  
351 significant. For the correction, we use lidar observations within up to 100 km distance and 60  
352 min time difference from the AMVs. A tighter criterion may be advisable for future  
353 applications, but in the current study this drastically limits the sample size and is therefore  
354 not shown.

355 The second part of the study compares AMV winds to layer-averaged radiosonde and  
356 dropsonde winds from T-PARC. Several layers of different depth are tested and these layers  
357 are shifted from above to beneath the AMV to investigate the depth of the layer that AMV  
358 winds represent and the appropriate position of such a layer relative to the original AMV



359 height. It is found that the VRMS differences are reduced by 5-10% when AMVs are assigned  
360 to a 100 hPa layer centered at their original height in comparison to a 10 hPa layer. Layer  
361 depths of 150-200 hPa lead to a slight further reduction of VRMS errors, but also tend to  
362 increase the bias of AMV-dropsonde wind speed differences. The optimal position of such a  
363 layer likely depends on the individual data set and the processing algorithm.

364 Our findings generally confirm that AMVs rather represent winds in a tropospheric layer  
365 than at a discrete level as demonstrated by VB2009 and emphasizes that AMVs should be  
366 assimilated as layer-wind in NWP models. Depending on the AMV channel and the  
367 geographical region, VB2009 suggest 50-150 hPa as appropriate layer depth for VIS, IR and  
368 SWIR AMVs, which is on average similar to our findings despite the different data set and  
369 methodology. In addition to VB2009, we demonstrated that treating AMVs as layer winds  
370 has no negative effect on systematic errors unless the averaging layers are significantly  
371 thicker than 100 hPa.

372 In summary, we conclude that the errors of T-PARC AMVs could be reduced by about  
373 5-10% when AMV winds were assigned to 100 hPa layers centered at their original height.  
374 Further error reduction by 10-15% could be reached when lower tropospheric AMVs were  
375 assigned to 100 or 150 hPa layers beneath the median height of nearby lidar cloud top  
376 observations and using 100 hPa layers centered at their original AMV height as reference.

377 The error reduction is demonstrated for a particular experimental AMV data set  
378 processed by CIMSS in one particular geographical region. The data set for the lidar height  
379 correction consists of 369 matches of AMV and lidar observations. Thus, results may be  
380 different for different regions, seasons and data sets. Nevertheless, it is demonstrated that  
381 lidar information can be used to determine AMV heights with reasonable accuracy and such

382 lidar observations constitute an independent and uncorrelated source of information. Thus,  
383 we think these results highlight the potential for reducing the errors and especially the error  
384 correlation of AMVs through the use of satellite lidar observations from CALIPSO or other  
385 spaceborne lidars in the future.

386

### 387 ***Acknowledgements***

388 AMV, lidar and dropsonde observations were made as part of T-PARC, TCS-08, and  
389 DOTSTAR. T-PARC and TCS-08 were sponsored by an international consortium from the  
390 United States (National Science Foundation, Office of Naval Research, Naval Research  
391 Laboratory, and U.S. Air Force), Germany (DLR, Forschungszentrum Karlsruhe), Japan (Japan  
392 Meteorological Agency), Korea (National Institute of Meteorological Research), and Canada  
393 (Environment Canada). The role of the National Center for Atmospheric Research's Earth  
394 Observing Laboratory (NCAR EOL) for campaign and data management is acknowledged.  
395 DOTSTAR is funded by the National Science Council of Taiwan, the United States Office of  
396 Naval Research, and the Central Weather Bureau Taiwan.

397 Particular thanks are due Oliver Reitebuch, Martin Wirth and Christoph Kiemle from the  
398 lidar group of the DLR Institute for Atmospheric Physics who supported the analysis of lidar  
399 observations and to Chris Velden and Steve Wanzong at CIMSS for processing the AMVs and  
400 providing information on the data set. The authors also want to acknowledge one  
401 anonymous reviewer, who made the important remark that AMVs should be compared to  
402 cloud heights derived from multiple lidar observations to avoid a mismatch of scales.

403 This study was carried out in the Hans Ertel Centre for Weather Research. This research  
404 network of universities, research institutes and Deutscher Wetterdienst is funded by the  
405 BMVBS (Federal Ministry of Transport, Building and Urban Development).

406

## 407 REFERENCES

408 Bormann, N., S. Saarinen, G. Kelly, and J.-N. Thépaut, 2003: The spatial structure of  
409 observation errors in atmospheric motion vectors from geostationary satellite data. *Mon.*  
410 *Wea. Rev.*, **131**,706-718.

411 Bormann, N. and J.-N. Thépaut, 2004: Impact of MODIS polar winds in ECMWF's 4DVAR data  
412 assimilation system. *Mon. Wea. Rev.*, **132**, 929-940.

413 Di Michele, S., T. McNally, P. Bauer, and I. Genkova, 2012: Quality assessment of cloud-top  
414 height estimates from satellite IR radiances using the CALIPSO lidar. *IEEE Trans. Geosci.*  
415 *Remote Sens.*, **PP**, 1-11, doi: 10.1109/TGRS.2012.2210721.

416 Harnisch F., M. Weismann, C. Cardinali, and M. Wirth, 2011. Assimilation of DIAL water  
417 vapour observations in the ECMWF global model. *Quart. J. Roy. Meteor. Soc.*, **137**, 1532–  
418 1546.

419 Gelaro, R., R. H. Langland, S. Pellerin, and R. Todling, 2010. The THORPEX observation impact  
420 inter-comparison experiment. *Mon. Wea. Rev.*, **138**, 4009-4025.

421 Folger, K., 2012: Höhenkorrektur von Satelliten-Windvektoren (AMVs) mit  
422 flugzeuggetragenen Lidarmessungen. Master thesis. Ludwig-Maximilians-Universität  
423 München, Germany. Online available at: <http://www.meteorologie.lmu.de/herz>

424 Nieman, S. J., J. Schmetz, and W. P. Menzel, 1993: A comparison of several techniques to  
425 assign heights to cloud tracers. *Journal of Applied Meteorology*, **32**, 1559-1568.

426 Olander, Z., 2001: UW-CIMSS satellite-derived wind algorithm user's guide (version 1.n).  
427 Online available at: <http://cimss.ssec.wisc.edu/iwwg/Docs/windcoug.pdf>

428 Velden, C. S., J. Daniels, D. Stettner, D. Santek, J. Key, J. Dunion, K. Holmlund, G. Dengel, W.  
429 Bresky, and P. Menzel, 2005: Recent Innovations in Deriving Tropospheric Winds from  
430 Meteorological Satellites. *Bull. Amer. Meteor. Soc.*, **86**, 205-223.

431 Velden, C. S., and K. M. Bedka, 2009: Identifying the Uncertainty in Determining Satellite-  
432 Derived Atmospheric Motion Vector Height Attribution. *J. Appl. Meteor. Climatol.*, **48**,  
433 450-463.

434 Weissmann M., F. Harnisch, C.-C. Wu, P.-H. Lin, Y. Ohta, K. Yamashita, Y.-H. Kim, E.-H. Jeon,  
435 T. Nakazawa, and S. Aberson, 2011. The influence of assimilating dropsonde data on  
436 typhoon track and mid-latitude forecasts. *Mon. Wea. Rev.* **139**, 908-920.

437 Weissmann, M., R. H. Langland, C. Cardinali, P. M. Pauley, and S. Rahm, 2012: Influence of  
438 airborne Doppler wind lidar profiles near Typhoon Sinlaku on ECMWF and NOGAPS  
439 forecasts. *Quart. J. Roy. Meteor. Soc.*, **138**, 118-130.

440 Wirth, M., A. Fix, P. Mahnke, H. Schwarzer, F. Schrandt, and G. Ehret, 2009: The airborne  
441 multi-wavelength water vapor differential absorption lidar WALES: System design and  
442 performance. *Appl. Phys.*, **96B**, 201-213.

	Difference of mean VRMS	Difference of absolute bias
IR, 100-499 hPa, 100 hPa layer centered at AMV	-0,36	-0,42
IR, 500-999 hPa, 100 hPa layer centered at AMV	-0,29	0,11
SWIR, 500-799 hPa, 100 hPa layer centered at AMV	-0,21	0,1
SWIR, 800-999 hPa, 100 hPa layer centered at AMV	-0,42	-0,09
VIS, 500-799 hPa, 100 hPa layer centered at AMV	-0,21	0,07
VIS, 800-999 hPa, 100 hPa layer centered at AMV	-0,24	-0,04
IR, 100-499 hPa, 50 hPa layer centered 16 hPa beneath AMV	-0,49	-0,5
IR, 500-999 hPa, 100 hPa layer centered 50 hPa above	-0,16	-0,08
SWIR, 500-799 hPa, 100 hPa layer centered 40 hPa above	-0,2	-0,38
SWIR, 800-999 hPa, 100 hPa layer centered 50 hPa beneath	-0,4	-0,11
VIS, 500-799 hPa	no suitable layer found	
VIS, 800-999 hPa, 100 hPa layer centered 50 hPa beneath	-0,44	-0,03

444

445 TABLE 1. Reduction of mean VRMS and wind speed bias (both  $\text{m s}^{-1}$ ) of differences between AMV and  
446 sounding winds when sounding winds are averaged over a layer described in the left column instead  
447 of a 10 hPa layer centered at the original AMV height. Negative values indicate lower values for the  
448 layer described in left column. The upper part of the table presents the results for 100 hPa layers  
449 centered at the original AMV height, the lower part the results for one other selected layer for every  
450 panel in Fig. 7.

451

452 **Figure captions**

453 FIG. 1. (left) Location of airborne Falcon observations used in section 3; lidar observations  
454 are represented by gray lines and dropsondes by black '+'-symbols; (right) location of  
455 soundings used in section 4; black '+'-symbols mark the location of dropsondes, circles mark  
456 special T-PARC radiosondes from ships or small islands. The size of circles representing  
457 sounding stations with more than 500 AMV matches used for the comparison is scaled  
458 linearly by the number of matches; the largest circle represents 1221 matches.

459 FIG. 2. (a) Height distribution of AMVs used for the lidar-AMV height comparison in section  
460 3a. (b) Height distribution of AMVs used for the height correction in section 3b.

461 FIG. 3. Histogram of height differences (hPa) between AMVs and lidar cloud top heights.  
462 Positive values indicate AMV heights that are lower than lidar cloud top heights.

463 FIG. 4. Relative reduction of mean AMV-dropsonde VRMS difference when AMVs are  
464 compared to a layer beneath the original AMV height instead of a layer centered at the  
465 original AMV height. The first three bars represent results for 50 hPa deep layers, the middle  
466 three bars for 100 hPa layers and the right three bars for 150 hPa layers.

467 FIG. 5. Mean VRMS and wind speed bias of differences between AMVs (VIS, IR and SWIR  
468 combined) and dropsondes when AMVs are assigned to a layer relative to nearby lidar cloud  
469 top observations. The x-axis denotes the depth of the assigned layer. The three different line  
470 types denote layers centered at the lidar cloud top (black dashed line), layers from the lidar  
471 cloud top downward (solid black line) and layers with 25% above and 75% beneath the lidar  
472 cloud top (solid gray line).

473 FIG. 6. Relative reduction of mean VRMS differences between AMV and dropsonde winds  
474 when AMVs are assigned to a layer beneath the lidar cloud top instead of a layer centered at  
475 the original AMV height. The depth of the layer is 100 hPa for the left bars and 150 hPa for  
476 the right ones.

477 FIG. 7. Mean VRMS and wind speed bias of differences between AMV winds and layer-  
478 averaged winds from dropsondes and radiosondes. The panel titles denote the AMV type  
479 (VIS, SWIR or IR), the height range of compared values in hPa and the number of compared  
480 values. Different line types represent different layer depths for the vertical averaging of  
481 dropsonde and radiosonde winds: gray dashed line for 10 hPa, gray solid line for 50 hPa,  
482 black dashed line for 100 hPa, black dash-dotted line for 150 hPa (panel (a) only) and black  
483 solid line for 200 hPa (panels (b)-(f)). Note that the scales for bias and mean VRMS values are  
484 different.

485

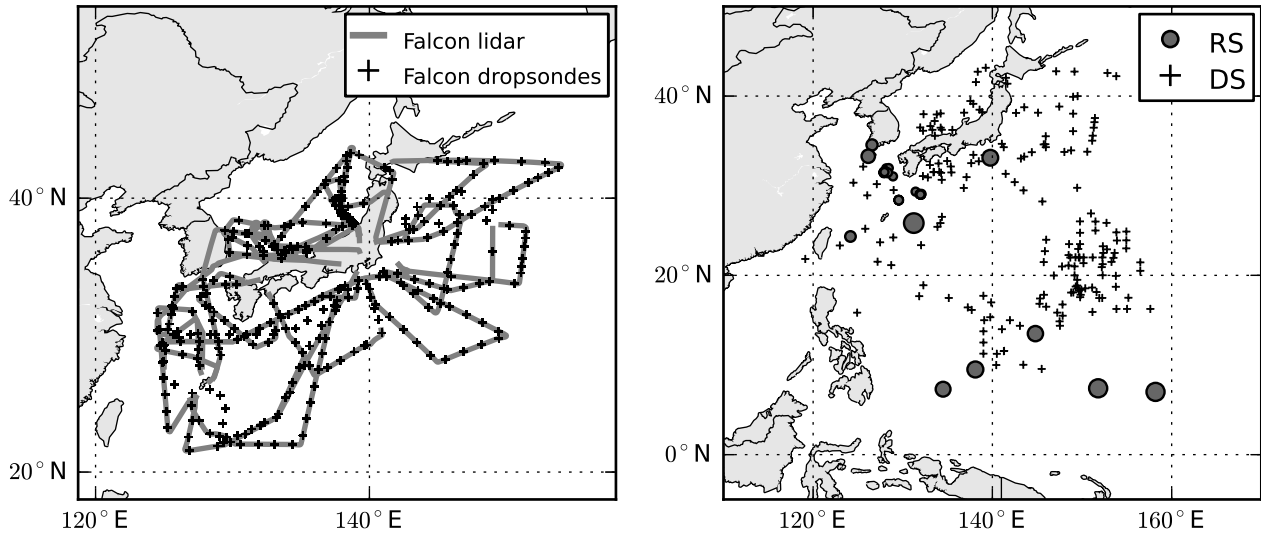


**FIG. 1.** (left) Location of airborne Falcon observations used in section 3; lidar observations are represented by gray lines and dropsondes by black '+'-symbols; (right) location of sounding used in section 4; black '+'-symbols mark the location of dropsondes, circles mark special T-PARC radiosondes from ships or small islands. The size of circles representing sounding stations with more than 500 AMV matches used for the comparison is scaled linearly by the number of matches; the largest circle represents 1221 matches.



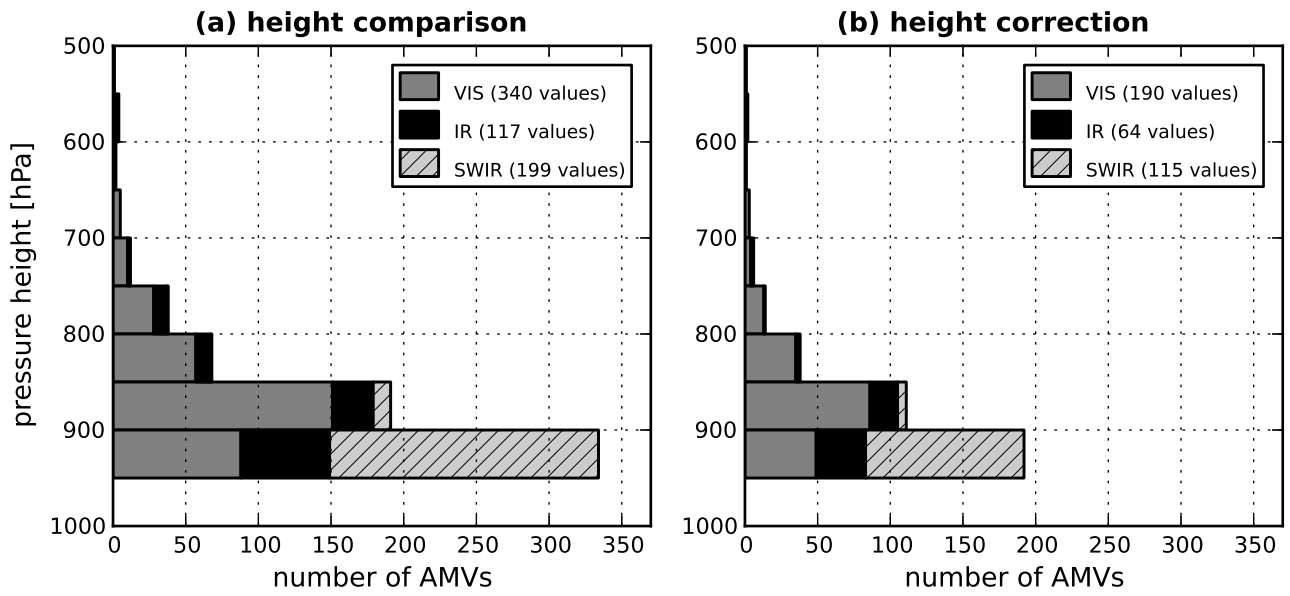


**FIG. 2.** (a) Height distribution of AMVs used for the lidar-AMV height comparison in section 3a. (b) Height distribution of AMVs used for the height correction in section 3b.

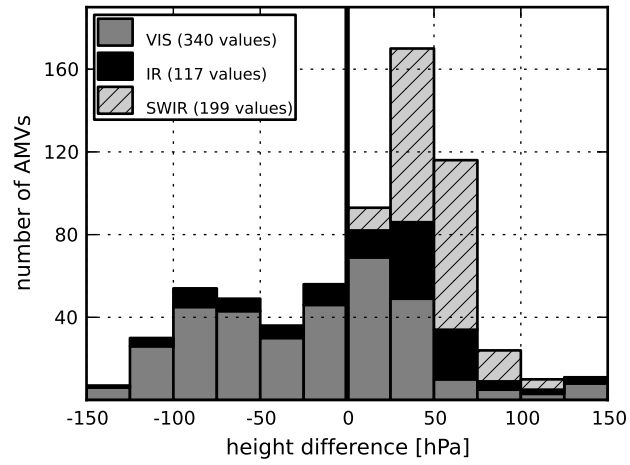


**FIG. 3.** Histogram of height differences (hPa) between AMVs and lidar cloud top heights. Positive values indicate AMV heights that are lower than lidar cloud top heights.

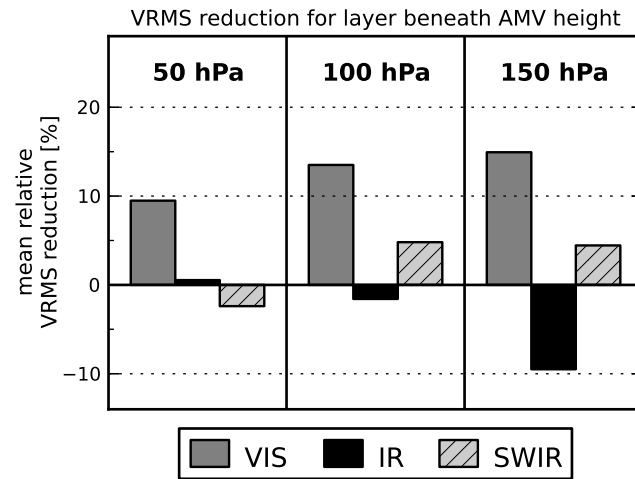


**FIG. 4.** Relative reduction of mean AMV-dropsonde VRMS difference when AMVs are compared to a layer beneath the original AMV height instead of a layer centered at the original AMV height. The first three bars represent results for 50 hPa deep layers, the middle three bars for 100 hPa layers and the right three bars for 150 hPa layers.

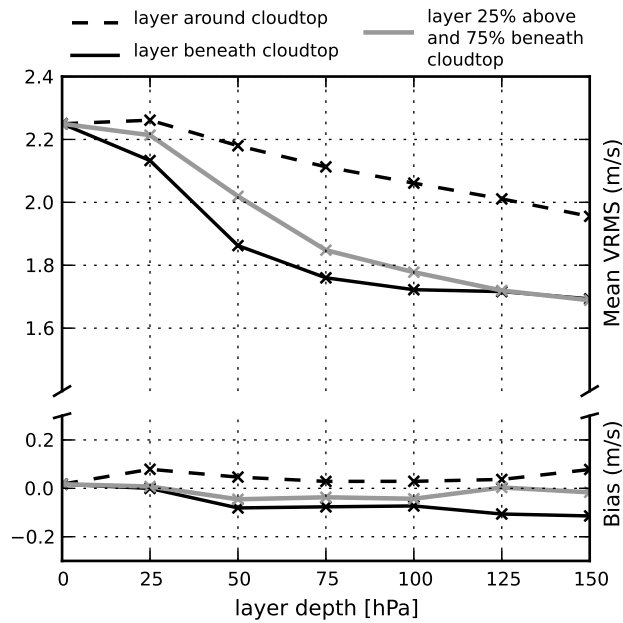


**FIG. 5.** Mean VRMS and wind speed bias of differences between AMVs (VIS, IR and SWIR combined) and dropsondes when AMVs are assigned to a layer relative to nearby lidar cloud top observations. The x-axis denotes the depth of the assigned layer. The three different line types denote layers centered at the lidar cloud top (black dashed line), layers from the lidar cloud top downward (solid black line) and layers with 25% above and 75% beneath the lidar cloud top (solid gray line).

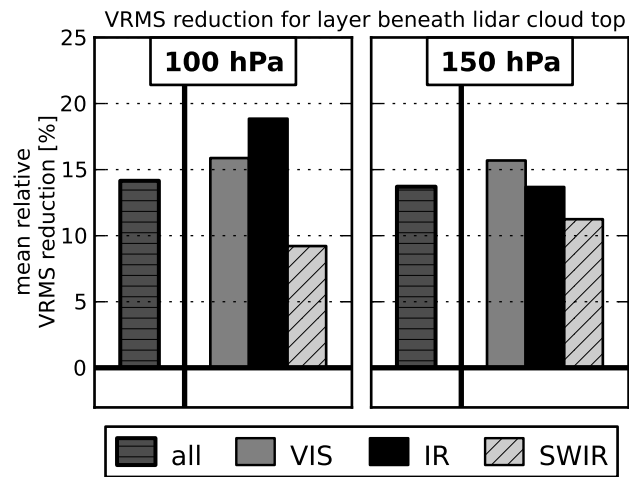


**FIG. 6.** Relative reduction of mean VRMS differences between AMV and dropsonde winds when AMVs are assigned to a layer beneath the lidar cloud top instead of a layer centered at the original AMV height. The depth of the layer is 100 hPa for the left bars and 150 hPa for the right ones.

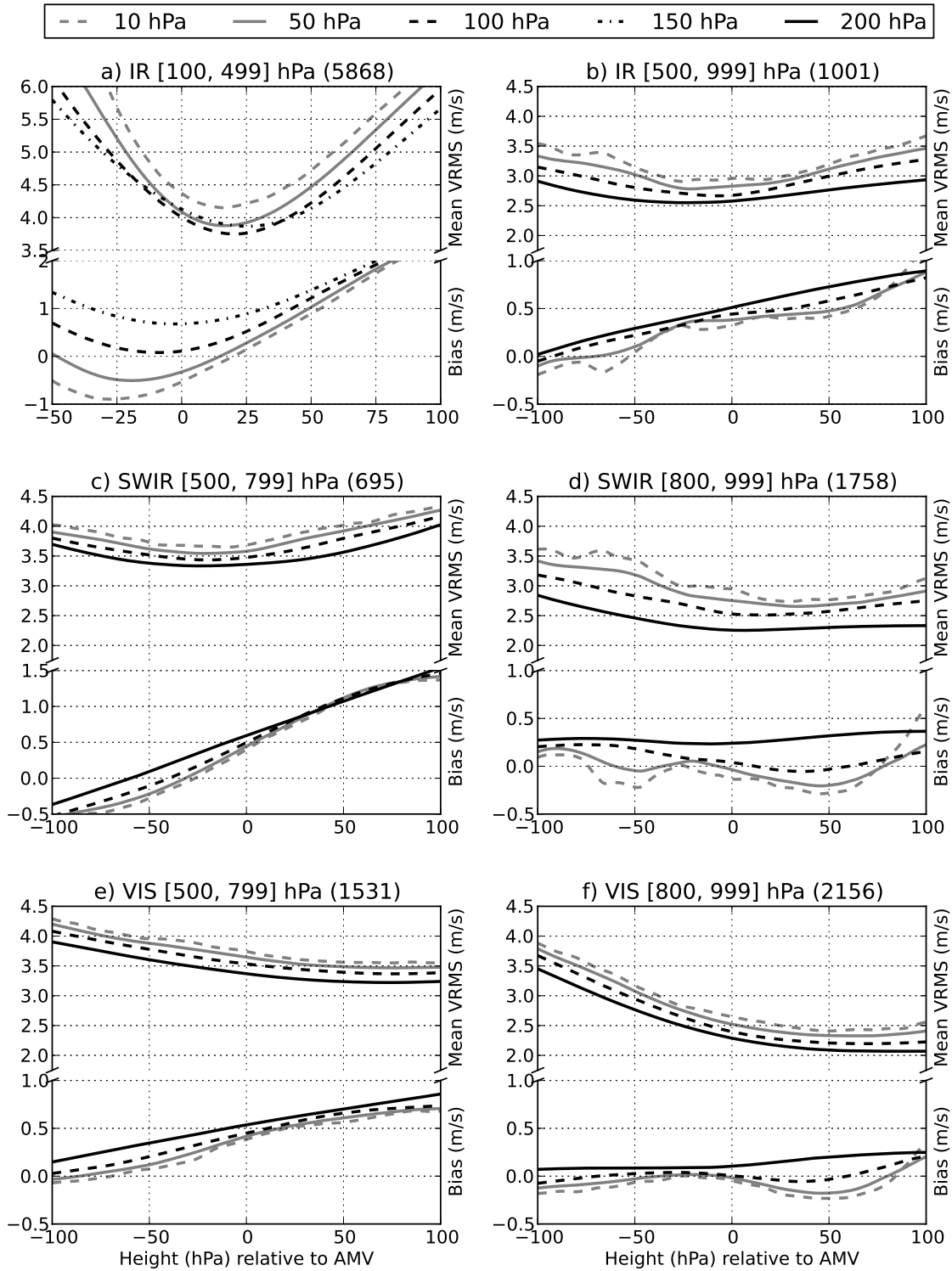


**FIG. 7.** Mean VRMS and wind speed bias of differences between AMV winds and layer-averaged winds from dropsondes and radiosondes. The panel titles denote the AMV type (VIS, SWIR or IR), the height range of compared values in hPa and the number of compared values. Different line types represent different layer depths for the vertical averaging of dropsonde and radiosonde winds: gray dashed line for 10 hPa, gray solid line for 50 hPa, black dashed line for 100 hPa, black dash-dotted line for 150 hPa (panel (a) only) and black solid line for 200 hPa (panels (b)-(f)). Note that the scales for bias and mean VRMS values are different.